L. A. Gilson

E. F. Harrold

F. G. Kilmer

Design Principles for Sampled-Data Systems with Application to Attitude Control of a Large, Flexible Booster

Abstract: This paper reviews Z-transform and W-transform theory and discusses in detail its application to dynamic compensation of linear sampled-data control systems. Both sampled-data (digital) and continuous-data (analog) compensator synthesis methods are discussed. With respect to digital compensator design, w-plane closed-loop pole positions are related to time response characteristics, analogous to the well known relationships between s-plane pole positions and time response parameters for continuous-data systems. An example is given which illustrates the design technique wherein time and frequency response characteristics are compared. A digital stabilization filter is derived for the attitude control system of a missile typical of the Saturn class.

Introduction

Fundamental digital filter theory has been well understood for some time. Its application to the aerospace industry is, however, of more recent origin, although digital controllers of both the conventional and the adaptive types have been considered extensively for flexible booster attitude control.^{1,2} Nevertheless, existing attitude control systems are essentially analog in nature. Although proven to be reliable in their operation, the design/fabriaction durations have been extremely long and stand to curtail future analog implementation. Detailed considerations are discussed herein which provide for efficient definition of digital stabilization filters. Digital programs have been written for general application of the design techniques to linear mixed-data systems characterized by "semi-slow," as well as fast, sampling and have been employed for the examples of this paper.

Theoretical review

A sampled-data system is characterized by the presence of one or more signals occurring at intermittent times. Sampling in physical systems occurs essentially in the form of signal sensing for a brief time interval, followed by a longer interval of no signal sensing. In the case of systems employing digital computers, sampling corresponds to the repetitive occurrence of a number for processing in an arithmetic fashion. Based on the fundamental assumption that the sampling interval is small in comparison to the time constants of the physical system under consideration,

a convenient mathematical description of the sampling process exists.³ As is generally known, the sampler model is referred to as an impulse modulator and establishes a one-to-one correspondence between the weighting of a train of impulse functions and the sequence of equally-spaced values of the signal being sampled.

In conventional mathematical notation, a sampled function of time may be expressed as

$$f^*(t) = \sum_{n=0}^{\infty} f(nT) \delta(t - nT), \qquad (1)$$

where f(t) represents the signal being sampled. One form of the Laplace transform of Eq. (1) is

$$F^*(s) = \frac{1}{T} \sum_{n=-\infty}^{+\infty} F(s + jn\omega_s), \qquad (2)$$

where $\omega_s = 2\pi/T$ is the sampling frequency. Equation (2) exhibits a well known property of discrete transfer functions. Since $F^*(s)$ is periodic in s with period $j\omega_s$, the poles and zeros of $F^*(s)$ are periodically distributed throughout the s-plane. Viewed geometrically, this periodicity occurs in the form of repeated strips in the s-plane, which are parallel to the real axis and ω_s in width. This is shown in Fig. 1, where the strip that is symmetrically oriented about the real axis is customarily referred to as the primary strip.

An alternate form for the Laplace transform of Eq. (1) is

$$F^*(s) = \sum_{n=0}^{\infty} f(nT)e^{-nsT}.$$
 (3)

The change of variable $z = e^{zT}$ allows Eq. (3) to be written as

$$F(z) = \sum_{n=0}^{\infty} f(nT)z^{-n},$$
 (4)

where $F(z) = F^*(1/T \ln z)$.

Equations (3) and (4) define the operation known as the Z-transform. A property of the change of variable $z=e^{sT}$ is that the primary strip in the s-plane maps into the entire z-plane with the left-half primary strip mapping into the interior of the z-plane unit circle. Furthermore, all other s-plane strips map into the z-plane in exactly the same manner. Although the apparent periodic pole-zero distribution has been removed, uniqueness between $F^*(s)$ and F(z) exists only if $(-\omega_s/2 + m\omega_s) < \omega \le (+\omega_s/2 + m\omega_s)$ and $(-\pi + m2\pi) < \arg z \le (\pi + m2\pi)$ where m is an integer. It may occur in practice that uniqueness is essentially preserved on the basis that the frequency range of interest is less than $\omega_s/2$. In this case, m is 0.

The response at the sample instants, c(nT), of a linear continuous (time-invariant) system G(s) to the input $F^*(s)$ is obtained from the inverse Z-transform as expressed by the contour integral

$$c(nT) = \frac{1}{2\pi j} \oint_{\Gamma} C(z) z^{n-1} dz, \qquad (5)$$

where the contour Γ encloses all of the poles of C(z) z^{n-1} . The derivation⁴ of Eq. (5) results in a range of z for which $-\pi < \arg z \le \pi$ or $-\omega_*/2 < \omega \le \omega_*/2$. That is, c(nT) is determined by the poles of $C^*(s)$ in the primary strip. This is to be contrasted with the inverse Laplace transform of C(s) as given by

$$c(t) = \frac{1}{2\pi i} \int_{\sigma - i\infty}^{\sigma + i\infty} F^*(s) G(s) e^{st} ds.$$
 (6)

It follows from the property that $F^*(s)$ is rational in e^{sT} (which is obtained from a closed form expression of Eq. (3)) that c(t) is determined by an infinite set of poles throughout the s-plane.

Expressing z^{n-1} as exp $[(1/T \ln z) (n-1) T]$ allows Eq. (5) to be written as

$$c(nT) = \frac{1}{2\pi j} \oint_{\Gamma} C(z) e^{(1/T \ln z) (nT - T)} dz.$$
 (7)

If nT is arbitrarily replaced by t, the integration will result in a continuous response $c_1(t)$ which is exactly equal to the time response c(t) at the sampling instants and approximately equal to c(t) at other than the sample instants. The importance of this substitution lies in the fact that the approximate response $c_1(t)$ may be readily characterized by the pole position of the dominant modes of $C^*(s)$ in the

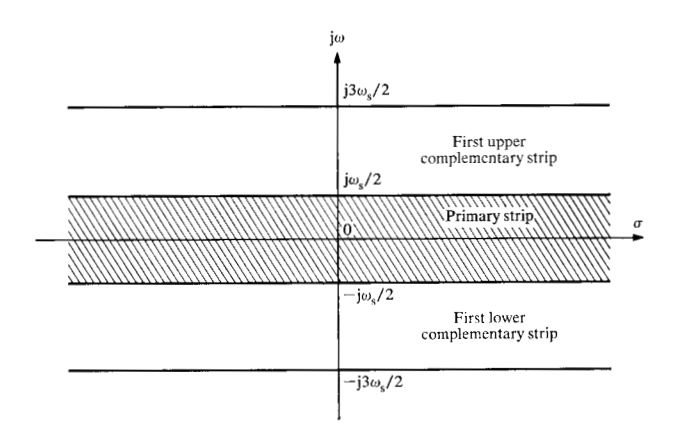


Figure 1 Periodic strips of width ω_s in the s-plane.

primary strip. The advantages of relating time and frequency domain parameters are well appreciated for continuous-data systems and prompted Johnson, Lindorff, and Nordling⁴ to propose the above substitution of t for nT. In this manner, time and frequency parameters are likewise related for the sampled-data problem. Johnson, et al have shown that the substitution of t for nT is justified if the frequency range of the system's dominant dynamics is $<\omega_e/2$. Methods employing the modified Z-transform and the convolution summation provide an exact determination of intersample response but do not readily permit the time-frequency domain correlation.

The W-transform has been proposed as a means to allow the use of all continuous-data compensation methods for sampled-data synthesis. The W-transform is defined by the change of variable z = (1 + w)/(1 - w). Thus,

$$w = \frac{z - 1}{z + 1} = \frac{e^{sT/2} - e^{-sT/2}}{e^{sT/2} + e^{-sT/2}} = \tanh \frac{sT}{2}.$$
 (8)

This bilinear transformation maps the interior of the z-plane unit circle into the entire left-half w-plane. This fact allows application of linear continuous-data system stability criteria to the corresponding sampled-data problem; i.e., Routh-Hurwitz, Nyquist, etc. Further, the $Z \rightarrow W$ -transformation produces transfer functions which are rational fractions in the variable of interest—frequency in the case of Bode and Nyquist methods application—thereby allowing use of asymptotic plotting techniques. For $s = j\omega$, the complex variable w = u + jv of Eq. (8) becomes u = 0 and

$$v = \tan \frac{\omega T}{2}. (9)$$

Equation (9) defines the scaling between the "real" frequency ω and the "fictitious" frequency v.

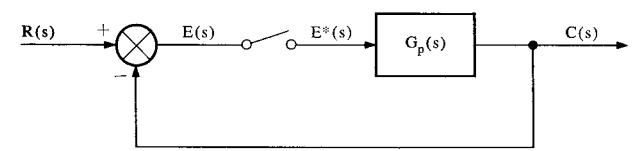
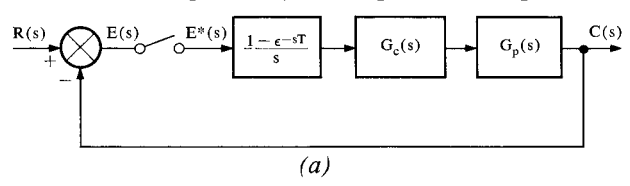
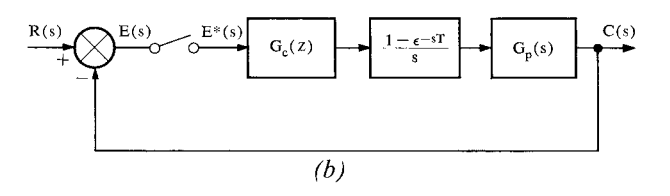


Figure 2 A basic sampled data control system.

Figure 3 Two methods of cascade compensation; (a) continuous-data compensation, (b) sampled-data compensation.





Design principles for compensation of sampled-data systems

A basic sampled-data control system with $G_p(s)$ representing the process to be controlled is shown in Fig. 2. It often occurs in practice that the dynamic performance of a given control system is inadequate and some means of compensation must be employed in order to result in acceptable system performance. In general, dynamic compensation is obtainable through introduction of an element either in series or in parallel with the given process. The former is referred to as cascade compensation and the latter as feedback compensation. Restricting attention to single-degree-of-freedom systems,5 there is no loss in generality, in terms of providing desired closed loop poles, by considering only cascade compensation. For sampleddata systems, there are two methods of achieving cascade compensation; either by continuous-data filters or discretedata filters. These two methods are shown in Figs. 3a and 3b, where, respectively, the sampled data is converted to continuous-data form prior to being operated on by the compensation filter $G_c(s)$, and the sampled data is operated on by a discrete filter $G_c(z)$ prior to data-form conversion. In reality, the discrete filter may be a continuous-data filter with a post sampler or an operation within a digital computer. In any event, the zero-order hold is a simple model for digital-to-analog data conversion.

Both sampled-data and continuous-data compensation methods are discussed in this paper. In the case of continuous-data compensator design, for the class of systems discussed in a later section, a sampled-data compensator is first obtained. The following discussion is, therefore, devoted to the subject of sampled-data compensation.

• Sampled-data compensation

In general, the design of a sampled-data compensator may be performed for linear dynamical systems described in either the s, z, or w variables. Frequency response and/or root-locus techniques are available in all three domains. As previously mentioned, absolute and relative stability criteria are essentially the same for transfer functions in s or w; therefore, stability properties may be readily evaluated in either domain. Frequency response methods for which $s = j\omega$ are, however, based on finite term approximation of an infinite summation, Eq. (2). Evaluation of absolute stability is directly apparent from a z-plane root locus plot; however, a determination of relative stability is obtainable only from a root locus analysis wherein the s-plane constant ζ and ω_n lines are mapped into the z-plane.

The w-plane approach is, therefore, favored by the authors for the convenience it provides in the form of frequency response locus shaping techniques, which are preferable for high-order (complex) systems design. Further, efficient and accurate implementation of frequency response locus determination, in the form of digital computer programs, may be constructed for systems described in z. To determine the $G^*(j\omega)$ locus, a natural logarithm must be evaluated (or an infinite series truncated for s-domain system description); whereas, to determine the $G(j\upsilon)$ locus, only an algebraic transformation is required.

For completeness of design methods in the w-domain, a technique for estimating the frequency and damping characteristics of the system time response is highly desirable. In the s-plane, a constant damping ratio ζ is represented by a straight line radiating from the orgin. The set of points in the w-plane which composes a constant ζ curve ($\zeta = \zeta_1$) is defined from Eq. (8) by

$$(u+jv)_{\zeta_1} = \frac{e^{\zeta_1 \omega_n T} e^{i(1-\zeta_1 z)^{1/2} \omega_n T} - 1}{e^{\zeta_1 \omega_n T} e^{i(1-\zeta_1 z)^{1/2} \omega_n T} + 1}.$$
 (10)

Figure 4 shows how the constant ζ lines in the s-plane map into curves in the w-plane. Geometrically, the fictitious damping ratio ξ represents in the w-plane the same quantity that ζ represents in the s-plane. Thus, constant ξ lines emanate radially from the origin in the w-plane, as shown in Fig. 4. Therefore, if the fictitious frequency v and damping ratio ξ are known, actual damping ζ may be obtained by inspection of Fig. 4, and real frequency ω , by direct transformation from v.

Alternately, Fig. 4 provides a means for determining the ξ value corresponding to desired damping ratio ζ of the $c_1(t)$ response. The ξ value is defined by the ξ line which

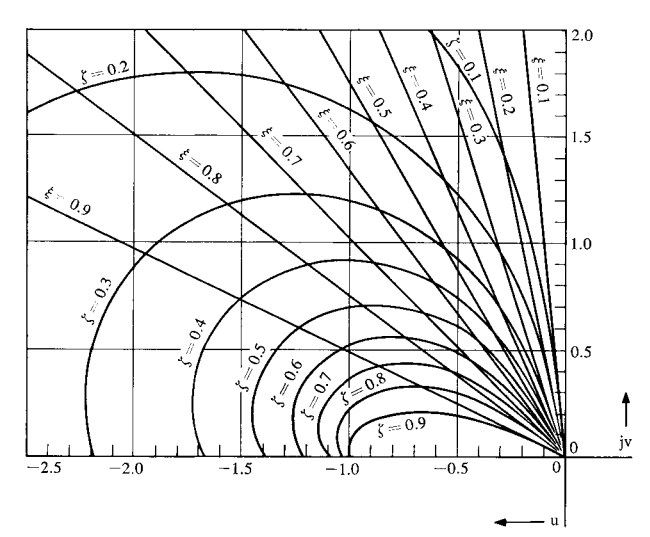


Figure 4 Mapping of constant ζ and constant ξ curves in w-plane.

intersects the desired ζ curve at the frequency, in v, of interest. Moreover, it is readily seen from the v- ω relationship that Fig. 4 provides a general design guide independent of the sample period T, which only determines the frequency scaling along the constant ζ curve.

If the M_p criterion is used as a means for providing desired damping of a dominant quadratic mode, the system frequency response locus P(jv) should be reshaped for tangency to the M_p curve defined by $M_p = 1/2\xi \sqrt{1-\xi^2}$. Should criteria other than M_p be employed for obtaining desired system relative stability via the w-plane synthesis, Fig. 4 provides equally useful information. For example, w-plane root locus plots can be used in conjunction with Fig. 4 to obtain a system design having desired damping and frequency of a particular mode or modes.

To illustrate application of the above discussed techniques to a practical system of interest, consideration is given to a missile attitude control system design.

• Example 1

Assume that the missile is a rigid body; no significant bending and sloshing dynamics. On the assumption that the actuator transfer function is unity, $G_{\nu}(s)$ of Fig. 5 includes only rigid body dynamics in a single plane—either pitch or yaw. The linear differential equations used to define rigid body rotational motion are (refer to next section):

Moment equation:

$$\ddot{\Phi} - c_1 \alpha + c_2 \beta = 0, \tag{11}$$

Angle relationship:

$$\alpha = \alpha_w + \Phi; \qquad \alpha_w = \frac{W}{V}.$$
 (12)

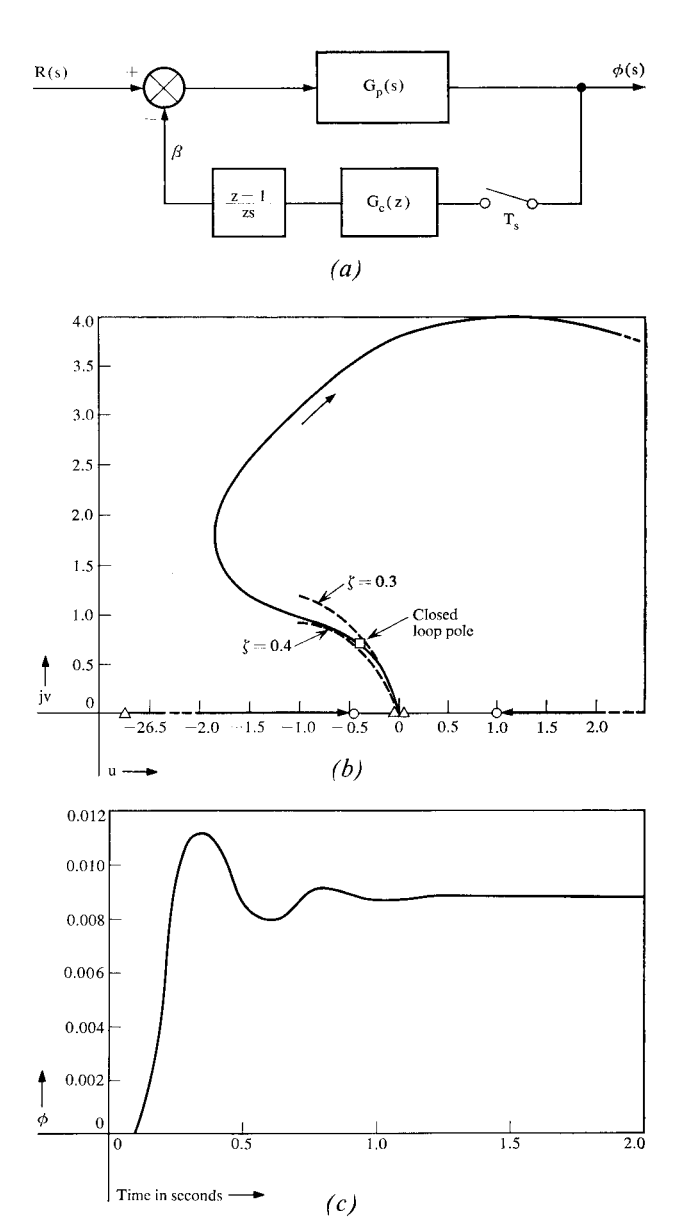


Figure 5 Example 1 system design; (a) block diagram, (b) w-plane root-locus of compensated system, (c) time response of system to step input.

Block diagram reduction of the above equations yields

$$G_{p}(s) = \frac{c_{2}}{s^{2} - c_{1}} \tag{13}$$

for Fig. 5 where $R(s) = (c_1/c_2)\alpha_w(s)$. Values representative of a large booster are $c_1 = 0.4187$ and $c_2 = 0.9363$. An open-loop pole exists at $\sqrt{c_1}$ and the plant is, therefore, unstable. Physically interpreted, this corresponds to the vehicle center of pressure being ahead of (with respect to the engine gimbal plane) the center of gravity. It will

be shown that feedback compensation, as illustrated in Fig. 5a results in a conditionally stable system.

A sampling frequency of 10 samples/second was selected. A rigid body mode damping of $0.3 < \zeta < 0.4$ at a damped natural frequency of approximately 12.75 radians per second (v = 0.74) was desired. The w-plane root-locus technique was used in conjunction with Fig. 4 to design a lead type digital compensator to stabilize the system. The following digital compensator was obtained:

$$G_c(w) = \frac{113.6\left(\frac{w}{0.45} + 1\right)}{\frac{w}{26.75} + 1},$$
(14)

or

$$G_c(z) = \frac{352.85(z - 0.3793)}{(z + 0.928)}. (15)$$

The w-plane root locus of the compensated system is shown in Fig. 5b. The $\zeta = 0.3$ and $\zeta = 0.4$ lines are superimposed on this plot to indicate satisfaction of that design objective. The time response of this system to a step input (r(t) = u(t); R(s) = 1/s) is presented in Fig. 5c. Inspection of the damping and frequency of this response offers further verification that the design objectives have been met.

This example clearly illustrates the relationship between w-plane pole positions and time response properties.

• Continuous-data compensation

From Fig. 3a, it is seen that the open-loop pulse transfer function is

$$\frac{C^*(s)}{E^*(s)} = \left[\frac{1 - e^{-sT}}{s} \cdot G_c(s) \cdot G_p(s)\right]^* \tag{16}$$

or equivalently

$$\frac{C^*(s)}{E^*(s)} = (1 - e^{-sT}) \left[\frac{G_c(s)G_p(s)}{s} \right]^*.$$
 (17)

Since $[G_1(s) \ G_2(s)]^* \neq G_1^*(s) \ G_2^*(s)$, the basic difficulty of continuous-data compensator synthesis for sampled-data systems is that $G_c(s)$ is trapped within the operation of obtaining a pulse transfer function. Stated differently, although the poles of $G_1G_2(s)$ are related to those of $G_1G_2(z)$ by the relationship $z=e^{sT}$, there is no simple analytic relationship between the zeros of $G_1G_2(s)$ and those of $G_1G_2(z)$, except for the special case where sampling is sufficiently fast to validate the small angle approximation of Eq. (8), yielding $T_1(s) = (1+sT/2)/(1-sT/2)$. Thus, even though a determination of relative stability may be obtained from a root

locus or Nyquist plot of $P_c^*(s) = C^*(s)/E^*(s)$ of Eq. (17), the effect of the compensator is dependent upon the parameters of $G_p(s)$. This greatly complicates the specification of an acceptable $G_c(j\omega)$. In fact, pursuing the problem in this manner amounts to synthesis on a trial-and-error basis.⁸

The approach taken herein generally parallels that contained in Kuo, 10 without the introduction of the r-transform and allows a direct solution of the continuous-data compensator problem for the class of systems represented by Fig. 3a. Let $P^*(s)$ denote the open-loop pulse transfer function of the uncompensated system; that is

$$P^{*}(s) = (1 - e^{-\sigma T}) \left[\frac{G_{p}(s)}{s} \right]^{*}. \tag{18}$$

It is assumed that an adequately compensated system loop transmission $P_c^*(s)$ may be defined through application of frequency response locus shaping or root locus techniques as previously discussed. Recognition that a zero-order hold precedes the compensator $G_c(s)$ in Fig. 3(a) suggests rewriting $P_c^*(1/T \ln z) = P_c(z)$ as

$$P_c(z) = \frac{z-1}{z} \left[\frac{z}{z-1} \cdot P_c(z) \right]$$
 (19)

From a partial fraction expansion of $P_c(z)/(z-1)$, there results

$$z \cdot \frac{P_c(z)}{z - 1} = \sum_i \frac{k_i z}{z - \alpha_i}$$
 (20)

It is known from basic Z-transform theory that

$$\sum_{i} \frac{k_{i}z}{z - \alpha_{i}} = Z \left[\sum_{i} \frac{k_{i}}{s + a_{i}} \right]$$
 (21)

where $Z[\Sigma_i (k_i)/(s+a_i)]$ denotes the Z-transform operation and $\alpha_i = \exp(-a_i T)$. From Eqs. (17), (19), and (20), it follows that

$$\left[\frac{G_c(s)G_p(s)}{s}\right]_{s=1/T \ln z}^* = \sum_i \frac{k_i z}{z - \alpha_i}.$$
 (22)

From Eqs. (21) and (22), one obtains

$$\frac{G_c(s)G_p(s)}{s} = \sum_i \frac{k_i}{s + a_i}$$
 (23)

If the frequency range of interest does not exceed $\omega_s/2$, it may be assumed that $a_i = (-\ln \alpha_i)/T$ with the imaginary part of a_i in the interval from $-\pi/T$ to π/T . By this assumption, a unique compensator is determined from solution of Eq. (23) for $G_c(s)$. In the event that $G_c(s)$ should prove to have a higher order numerator than denominator, physical realizability may be established by addition of a pole(s) with sufficiently large real part.

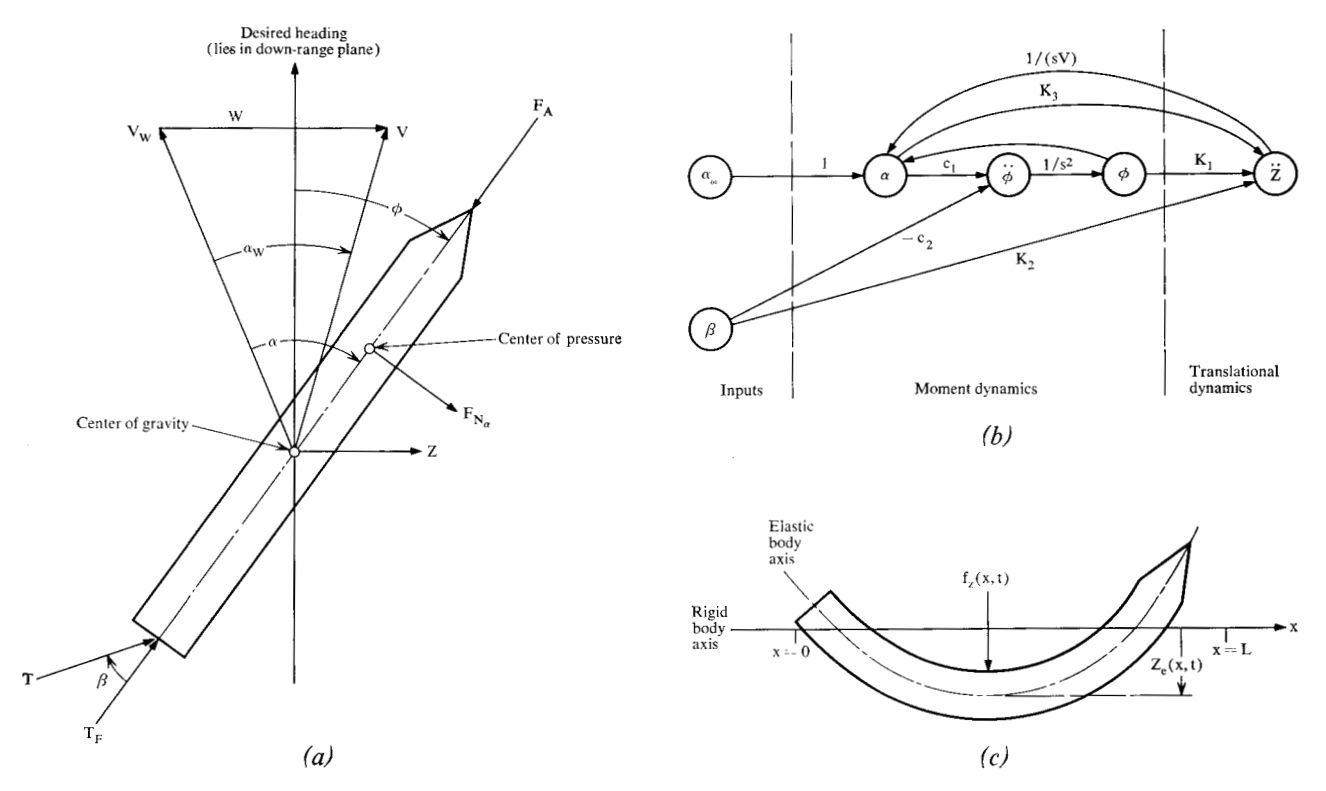


Figure 6 Dynamics of a large, flexible booster; (a) force and angle variables of rigid-body missile in flight, (b) signal flow graph of rigid-body dynamics, (c) bending variables.

Booster attitude control

The approach taken to design of an ascent-to-orbit attitude control system entails linear time invariant system analysis referenced to a number of flight time operating points, followed by analog (and digital) simulation studies for final design and evaluation purposes. This requires the derivation of linear (perturbation) differential equations describing the dynamical properties of the missile in the neighborhood of expected flight conditions. Such mathematical models, to various degrees of sophistication, have long been in existence; 11.12 however, the development of a basic set of equations will now be concisely summarized as a prelude to statement of a control system design problem for which a digital controller is required.

Figure 6a illustrates the aerodynamic and thrust forces acting on a rigid missile in atmospheric flight along with the pertinent orientation variables. As shown, the illustration actually pertains to lateral, or yaw, motion. As such, yaw component of attitude error is represented by φ and the wind W is the lateral component of total wind. Further, V represents the missile inertial velocity and F_N and F_A are the normal and axial aerodynamic forces acting on the vehicle through the center of pressure. On the assumption that pitch, yaw and roll motions are uncoupled, the linear perturbation (subject to small angle approximation)

equations of motion are seen to be

Moment equation:

$$\ddot{\varphi} = c_1 \alpha - c_2 \beta; \qquad c_1 = \frac{F_{N_\alpha} l_\alpha}{I_{yy}}, \qquad c_2 = \frac{T l_\beta}{I_{yy}} \quad (24)$$

Force equation:

$$\ddot{Z} = K_1 \varphi + K_2 \beta + K_3 \alpha \tag{25}$$

Angular relationship:

$$\frac{\dot{Z}}{V} = \varphi - \alpha + \alpha_w; \qquad \alpha_w = \frac{W}{V}. \tag{26}$$

In these equations, α denotes the missile angle of attack and β represents the thrust deflection of an equivalent single control engine. The K_i 's are thrust to mass ratios; $I_{\nu\nu}$ is the yaw moment of inertia; and l_{α} and l_{β} are moment arms. A signal flow graph of the rigid body equations is shown in Fig. 6b. It is seen that as $Z/V \rightarrow 0$, the feedback from Z to α is essentially open. In this case, the rotational motion affects the translational motion, but is unaffected by it. The translational motion is often referred to as the path root mode and is generally ignored in attitude control system design and stability analyses on the premise that $Z/V \cong 0$. (The equations of motion in the pitch plane are

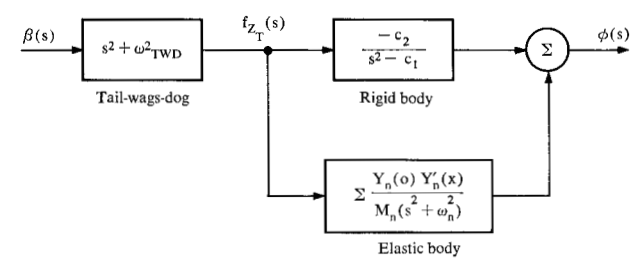


Figure 7 Block diagram of system dynamics

identical due to missile symmetry about its longitudinal, or roll, axis.)

A derivation of body bending dynamics will now be summarized.¹² The elastic body deformation $Z_{\epsilon}(x, t)$, shown in Fig. 6c as being superimposed on the rigid body motion, is defined by

$$\frac{\partial^{2}}{\partial x^{2}} \left[EI(x) \frac{\partial^{2} Z_{\bullet}}{\partial x^{2}} \right] + m(x) \frac{\partial^{2} Z_{\bullet}}{\partial t^{2}} = F_{Z}(x, t), \qquad (27)$$

subject to the boundary conditions

$$\frac{\partial^2 Z_{\epsilon}}{\partial x^2} = \frac{\partial^3 Z_{\epsilon}}{\partial x^3} = 0, \quad \text{for} \quad x = 0, \qquad x = L.$$
 (28)

The normal force distribution on the missile, in the attitude plane of interest, is assumed to consist of a control force concentrated at the base of the missile (x = 0) and a distributed aerodynamic force F_{Z_N} . Thus

$$F_z(x, t) = F_{z,z}(t) \delta(x) + F_{z,y}(x, t),$$
 (29)

where $\delta(x)$ is the unit dirac-delta function.

The Laplace transform of Eq. (27) with respect to t yields the ordinary differential equation

$$\frac{d^2}{dx^2}\left[EI(x)\frac{d^2(x,s)}{Z_{\epsilon}dx^2}\right] + s^2m(x)Z_{\epsilon}(x,s) = F_Z(x,s).$$
(30)

The homogenous form of Eq. 30, $F_Z(x, s) = 0$, has a nontrivial solution consisting of an infinite set of orthogonal eigenfunctions $Y_n(x, \lambda_n)$ with a corresponding set of eigenvalues λ_n . The general solution of Eq. (30) is, therefore,

$$Z_{e}(x, s) = \sum_{n=1}^{\infty} A_{n}(s) Y_{n}(x, \pm j\omega_{n}), \qquad (31)$$

where $\omega_n = \sqrt{\lambda_n}$. The functions Y_n are the body bending mode shapes and ω_n are the bending frequencies. Upon substitution of the general solution into Eq. 30, manipulation, and integration over the body length, there results

$$A_n(s) \cong \frac{Y_n(0)}{M_n} \frac{F_{Z_T}(s)}{(s^2 + \omega^2)},$$
 (32)

based on the approximation that the integral over the length of the missile of $F_{Z_N}(x, s)$ $Y_n(x)$ is zero. With respect to Eq. (32)

$$M_n = \int_0^L m(x) Y_n^2(x) dx$$
 (33)

is defined as the generalized mass of the *n*th bending mode. The net result is the transfer function from control thrust to vehicle attitude, due to body bending, of

$$\frac{\varphi_{e}(x,s)}{F_{Z_{T}}(s)} = \sum_{n=1}^{\infty} \frac{Y_{n}(0) Y_{n}'(x)}{M_{n}(s^{2} + \omega_{n}^{2})}; \qquad \varphi_{e} = \frac{dZ_{e}}{dx}$$
(34)

In practice, a slight amount of structural damping is assigned to each bending mode—usually of the order of $\zeta_n = 0.01$ to 0.05.

Additional dynamics exist due to nonzero engine mass for gimballed engines. A simple summation of forces normal to the missile axis for the engine free body yields the transfer function.

$$\frac{F_{ZT}}{\beta}(s) = (s^2 + \omega_{TWD}^2); \qquad \omega_{TWD}^2 = \frac{T}{S_{\bullet}}, \qquad (35)$$

where the anti-resonance factor is commonly referred to as the tail-wags-dog term. Equation (35), wherein S_{ϵ} denotes the engine mass moment, represents a simplified form of tail-wags-dog which is common to both rigid and elastic body dynamics.

Figure 7 shows a block diagram of dominant missile dynamics; translational and liquid fuel slosh dynamics have been ignored.

• Attitude control system design

Having defined the linear differential equation description of the dynamics of a large booster, consider now the application of the aforementioned w-plane techniques to the design of the digital compensator. Many present control schemes basically consist of attitude and attitude rate feedback with continuous-data compensators in both the attitude rate and attitude error channels. Sensed vehicle attitude is sampled prior to comparison with commanded heading; i.e., attitude error is defined in discrete form prior to digital-to-analog conversion. It is, therefore, realistic to consider employing a single digital controller in the attitude error channel, as illustrated in Fig. 8.

Assume the vehicle dynamics to consist of tail-wags-dog, rigid body, and six bending modes. In addition, a third-order linear actuator model is included, resulting in an uncompensated system of order 14/17. For the purpose of specifically illustrating the digital compensator design technique, consider a sampling frequency of 12.5 cps.

The over-all objective of the design is to obtain a digital compensator $G_c(z)$ which, when implemented as shown in Fig. 8, will assure the desired performance of the system

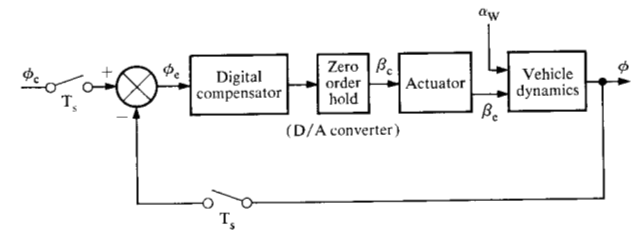


Figure 8 Attitude control system using digital attitude error-channel compensation.

plant just described. For the classical second-order continuous-data system, the stability margins necessary to achieve the desired time response characteristics are determined from known relationships which exist between time response and frequency response phase and gain margins. However, for high-order systems, no simple relationships exist between time and frequency response characteristics. For systems of this complexity, familiarity with the problem indicates the stability margins necessary for acceptable system performance. The exact analogous situation exists for the design in the w-domain; Fig. 4 defines the design requirements for low-order systems; problem familiarity is required for high-order systems. For the sake of design illustration, the following design objectives are given:

- ±6 dB of gain margin on the conditionally stable rigid body mode.
- 2. A minimum of 30 degrees phase margin on the rigid body mode.
- The control or rigid body natural frequency should be 0.2 to 0.4 cps.
- 4. Phase stabilization (stable regardless of gain) of the lowest frequency bending mode with minimum phase margins of ±60 degrees. (Phase stabilization of the first bending mode facilitates maximizing system bandwidth.)
- Gain stabilization (stable regardless of phase) of the remaining bending modes with a minimum of 12 dB attenuation.

The (uncompensated) open loop frequency response, $\Phi/\beta_c(jv)$, for vehicle parameters typical of a large booster at a critical flight time are presented in Figs. 9a and 9b. The corresponding Nyquist plot is shown in Fig. 10. Detailed examination of these responses indicates:

- 1. There is one clockwise encirclement of -1.0 point. Based on the Nyquist criterion, one counterclockwise encirclement is required for closed loop stability due to the unstable rigid body mode discussed in Example 1.
- 2. All six bending modes are gain stabilized. The least attenuated is the first bending mode which has a peak

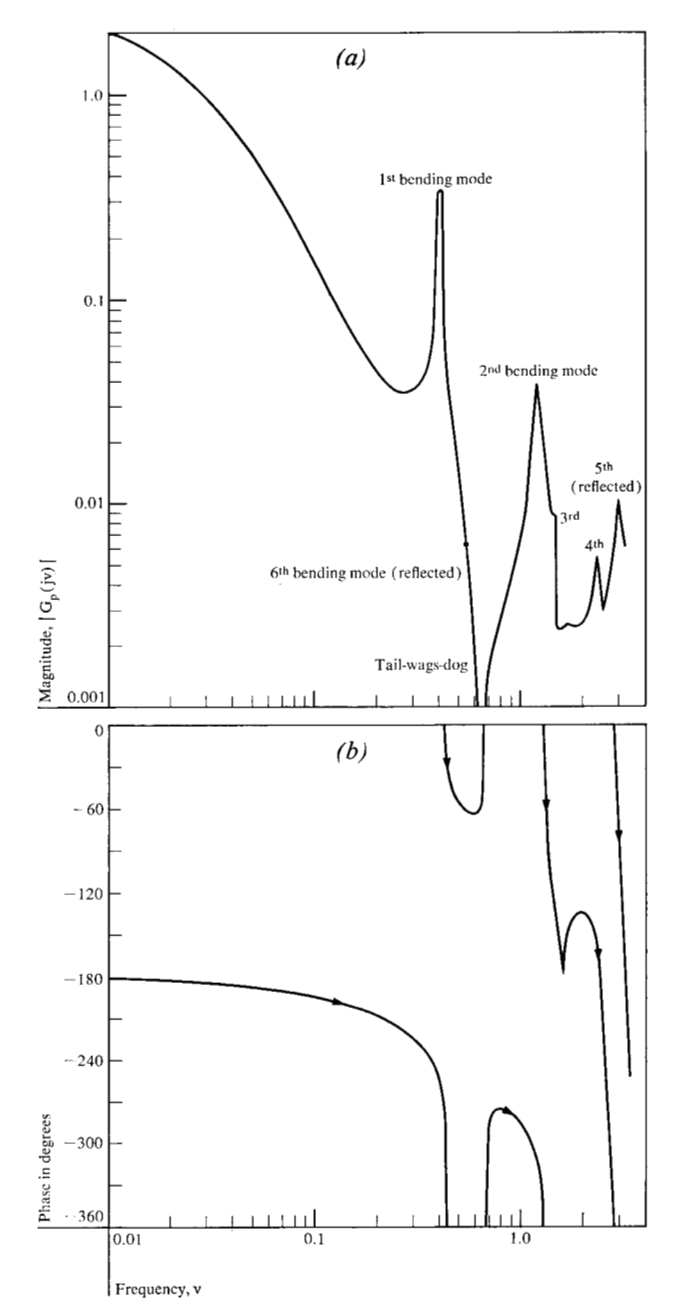


Figure 9 Open-loop frequency response of booster attitude control system; (a) magnitude vs frequency, (b) phase vs frequency.

amplitude of 0.47; all of the remaining modes are attenuated more than 20 dB. Although two high-frequency bending modes were reflected into the $-\omega_*/2 \le \omega \le \omega_*/2$ frequency range by the sampling process, their effect on the system frequency response is insignificant.

3. The tail-wags-dog anti-resonance occurs at a v frequency of 0.65 for this particular plant.

Based on these factors, the following modifications to the system frequency response are necessary for satisfaction of the aforementioned design specifications:

- At least 35 degrees phase lead is necessary in the low-frequency (rigid body) range. The associated increase in system gain will result in the desired +6 dB gain margin for the rigid body mode and also increase its natural frequency, as seen from Fig. 9a. However, the peak magnitude of the first bending mode will also be amplified.
- To prevent first bending mode resonance, sufficient phase lag must be introduced in the vicinity of this mode to attain phase stabilization—at least ±60 degrees phase margin.
- 3. To suppress the effects of all higher bending modes, increased attenuation is desirable in the high frequency range.

In summary, compensator requirements are: phase lead and amplification in the low frequency range; phase lag in the first bending mode frequency range; and maximum attenuation in the higher bending mode frequency range. Figure 11 illustrates the frequency response of an acceptable compensator, and Fig. 12a shows the *w*-plane Nyquist of the compensated system. The *w*-plane and *z*-plane response of the compensator are given, respectively, by

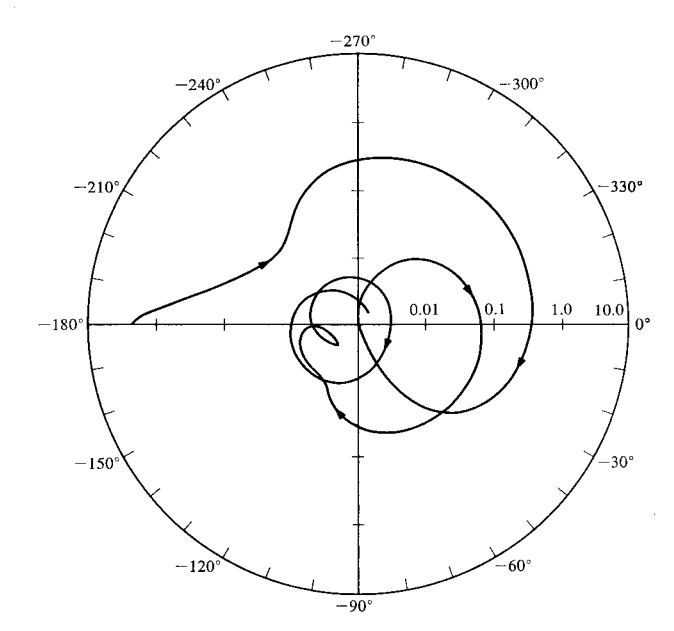


Figure 10 w-plane Nyquist plot of open-loop system.

$$G_c(w) = \frac{(1.365)\left(\frac{w}{0.034} + 1\right)\left[\frac{w^2}{(0.28)^2} + \frac{2(0.26)}{(0.28)}w + 1\right]}{\left(\frac{w}{0.32} + 1\right)\left[\frac{w^2}{(0.32)^2} + \frac{2(0.42)}{(0.32)}w + 1\right]\left[\frac{w^2}{(0.39)^2} + \frac{2(0.33)}{(0.39)}w + 1\right]}, \text{ and}$$
(37)

$$G_c(z) = \frac{1.246(z^2 - 1.50078z + 0.76186)(z - 0.93426)(z + 1.0)^2}{(z^2 - 1.31015z + 0.60702)(z^2 - 1.19947z + 0.63636)(z - 0.51685)}.$$
(38)

The time response of the compensated system to a step in α_w (wind disturbance) was obtained through digital simulation and is shown in Fig. 12b. Further verification of the design acceptability is evidenced in the characteristics of this response.

The preceding design has served to illustrate the application of W-plane frequency response techniques to digital compensator definition for a complex system. This design represents a first, but important, step in an over-all design procedure. Simulation studies and implementation considerations are necessary supplements to linear system design. Pertinent system nonlinearities and the effects of time varying parameters may be evaluated through simulation. Compensator synthesis, desired signal conditioning, and data form (discrete, continuous) conversion characteristics require definition. For example: computer programming of the digital filter must generally be oriented

to minimal computing requirements; presampler low pass filtering, as a means to eliminate the reflection of significant high frequency dynamics, is an important practical consideration.

Conclusions

Basic principles for efficient definition of stabilization filters for sampled-data systems have been presented. w-plane design techniques for sampled-data systems were emphasized because of the resultant convenience they afford for dynamic compensation of complex systems. Important relationships between frequency (w = jv) and time responses were presented. A technique which directly defines a continuous-data compensator for a sampled-data system was discussed.

Application of W-plane design techniques resulted in an estimate of digital stabilization filter complexity for a

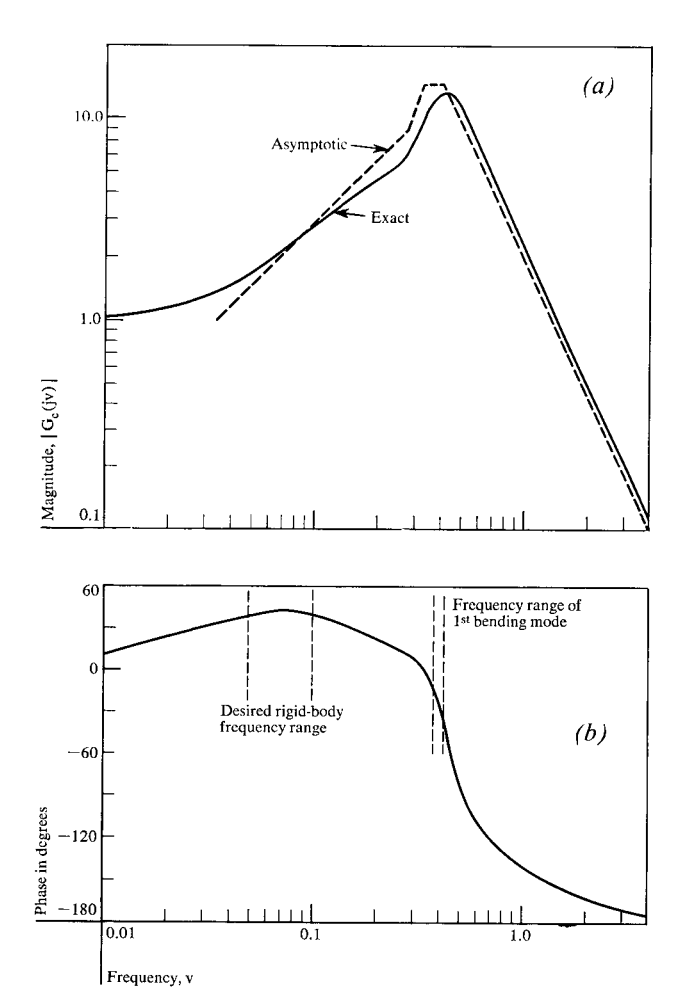


Figure 11 Frequency response of compensator; (a) magnitude vs frequency, (b) phase vs frequency.

large booster vehicle. Although certain system implementation problems remain to be solved, the estimate does provide a basis for determination of computing requirements.

Acknowledgment

The authors wish to thank Dr. G. W. Johnson for his suggestions and encouragement.

References

- G. W. Johnson, and F. G. Kilmer, "Saturn SA-1 Flight Control Study," IBM Report No. 65-816-0472, October 25, 1961.
- J. C. Blair, J. A. Lovingood, and E. D. Geissler, "Advanced Control Systems for Launch Vehicles," Astronautics & Aeronautics, August 1966.
- W. K. Linville, Notes from "Pulsed-Data Systems Course," Massachusetts Institute of Technology, Second Term, 1957.
- 4. G. W. Johnson, G. P. Lindorff, and C. G. A. Nordling, "Extension of Continuous-Data System Design Techniques to Sampled-Data Control Systems," *Trans. AIEE* 74, Pt. II, 252–263, (1955).

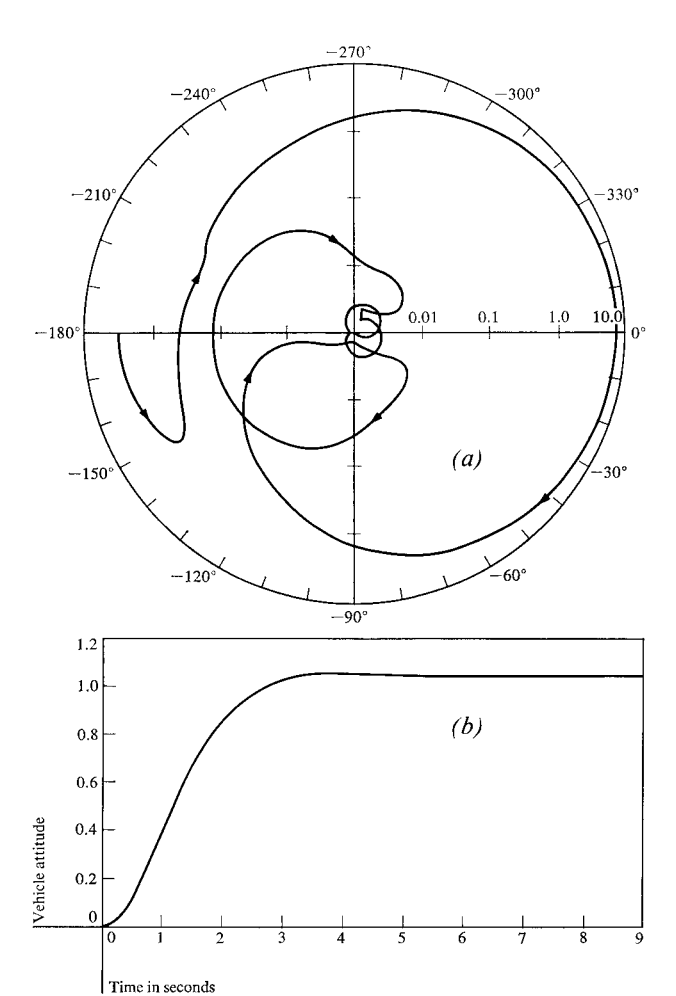


Figure 12 Compensated attitude control system; (a) Nyquist plot, (b) time response to step-function wind disturbance, α_w .

- I. M. Horowitz, "Synthesis of Feedback Systems," Academic Press, New York & London, Chap. 5. 1963.
- C. J. Savant, "Basic Feedback Control System Design," McGraw-Hill Book Co., Inc., New York, Toronto, & London, Appendix VIII, 1958.
- D. P. Lindorff, "Theory of Sampled-Data Controls Systems," John Wiley & Sons, Inc., New York, London, & Sydney, Sec. 3.8, 1965.
- 8. E. I. Jury, "Sampled-Data Control Systems," John Wiley & Sons, Inc., New York & London, Chap. 6, 1958.
- J. T. Tou, "Digital and Sampled-Data Control Systems," McGraw-Hill Book Co., Inc., New York, Toronto, & London, Chap. 9, 1959.
- B. C. Kuo, "Analysis and Synthesis of Sampled-Data Control Systems," Prentice Hall, Inc., Englewood Cliffs, New Jersey, Sec. 8. 3, 1963.
- 11. E. D. Geissler, "Problems in Attitude Stabilization of Large Guided Missiles," *Aerospace Engineering*, pp. 24–29, 68–72, (October, 1960).
- F. G. Kilmer, and G. W. Johnson, "Marp Report on Ballistic Missile Flight Control Theory," IBM Report No. 60-504-48, January 16, 1961.

Received October 17, 1966